Liquid-infiltrated photonic crystals: Ohmic dissipation and broadening of modes

Niels Asger Mortensen
nam@mic.dtu.dk

MIC – Department of Micro and Nanotechnology, NanoDTU, Technical University of Denmark, DTU–building 345 east, DK–2800 Kongens Lyngby, Denmark

Simon Ejsing

MIC – Department of Micro and Nanotechnology, NanoDTU, Technical University of Denmark, DTU–building 345 east, DK–2800 Kongens Lyngby, Denmark

Sanshui Xiao
Sanshui.Xiao@mic.dtu.dk

MIC – Department of Micro and Nanotechnology, NanoDTU, Technical University of Denmark, DTU–building 345 east, DK–2800 Kongens Lyngby, Denmark

The pronounced light–matter interactions in photonic crystals make them interesting as opto–fludic "building blocks" for lab–on–a–chip applications. We show how conducting electrolytes cause dissipation and smearing of the density–of–states, thus altering decay dynamics of excited bio–molecules dissolved in the electrolyte. Likewise, we find spatial damping of propagating modes, of the order dB/cm, for naturally occurring electrolytes such as drinking water or physiological salt water. [DOI: 10.2971/jeos.2006.06032]

Keywords: Optofluidics, photonic crystals, density–of–states, electrolytes

1 Introduction

With the emerging field of opto–fluidics [1] there is an increasing attention to liquid–infiltrated photonic crystals and the development has to a large extend been powered by their potential use as bio–chemical sensors [2]–[9]. Generally speaking, photonic crystals are strongly dispersive artificial materials, first suggested in 1987 by Yablonovitch [10] and John [11], where a periodic modulation of the dielectric function causes strong light–matter interactions for electromagnetic radiation with a wavelength comparable to the periodicity of the material. Typically, photonic crystals are made from a high–index dielectric with a periodic arrangement of voids. Alternatively, free–standing high–index dielectric structures may be utilized.

From a sensing point of view, light is an often utilized probe in analytical chemistry and for miniaturized lab–on–a–chip implementations, combining microfluidics [12, 13] and optics, there is a strong call for enhanced light–matter interactions compensating for the reduced optical path length. Liquid–infiltrated photonic crystals are obvious candidates for this where e.g. Beer–Lambert–Bouguer absorbance cells may benefit from slow–light phenomena [14]. Alternatively, weak perturbations in the liquid refractive index may cause considerable shifts in electromagnetic modes, thus making liquid–infiltrated photonic crystals promising candidates for refractometry [9].

Most bio–chemistry quite naturally occurs in the liquid phase and typically the host environment is a conducting electrolyte. In fact, even highly purified water will be weakly conducting due to the dissociation of water molecules (H_2O) into hydrogen (H^+) and hydroxide (OH^-) ions. In this paper we con-

sider the effect of Ohmic dissipation and broadening of levels in liquid infiltrated photonic crystals.

2 THEORY

We first consider the general case of a photonic crystal where the unit–cell of the periodic structure is composed of a solid high–index dielectric (d) material surrounded or infiltrated by a liquid (l). The corresponding relative dielectric function is given by

$$\varepsilon(\boldsymbol{r}) = \begin{cases} \varepsilon_d & , \quad \boldsymbol{r} \in \mathscr{V}_d, \\ \varepsilon_l + i\frac{\sigma}{\omega} & , \quad \boldsymbol{r} \in \mathscr{V}_l. \end{cases} \quad (1)$$

where the complex dielectric function of the liquid is quite similar to the Drude model often employed for the response of metals at optical frequencies. For liquids it is an adequate description of bulk properties, thus neglecting possible surface chemistry and Debye–layer ion accumulation at the interfaces to the high–index material. Electro–hydrodynamics where momentum is transferred from the ionic motion to the fluid (see e.g. Ref. [15] and references therein) is also strongly suppressed for optical frequencies, since the Debye screening layer forms too slowly in respond to the rapidly varying optical field. It is common to introduce the Debye response time $\tau_D = \omega_D^{-1} = \varepsilon_l/\sigma$ and for typical electrolytes, τ_D is less than a micro second corresponding to a Debye frequency in the megahertz regime. For optical frequencies, $\omega \gg \omega_D$, it is thus fully adequate to treat the imaginary part in Eq. (1) perturbatively. The unperturbed electromagnetic modes are governed by the following generalized eigenvalue problem for the elec-

trical field

$$\nabla \times \nabla \times |E_m\rangle = \epsilon \frac{\omega_m^2}{c^2} |E_m\rangle \qquad (2)$$

where ω_m is the eigenfrequency of the mth mode, c is the speed of light in vacuum, and $\epsilon(r) = \lim_{\sigma \to 0} \epsilon(r)$ is the unperturbed dielectric function characterizing the electromagnetic problem in the absence of conduction. In the following the unperturbed eigenmodes are normalized according to $\langle E_n | \epsilon | E_m \rangle = \delta_{nm}$ where δ_{nm} is the Kroenecker delta. From standard first–order perturbation theory, the effect of a finite conductivity leads to an imaginary shift in the frequency,

$$\Delta\omega_m = -\frac{\omega_m}{2} \frac{\langle E_m | i \frac{\sigma}{\omega_m} | E_m \rangle_{\mathscr{V}_l}}{\langle E_m | \epsilon | E_m \rangle_{\mathscr{V}_{l+d}}} \qquad (3)$$

where the integral in denominator is restricted to the liquid region $\mathscr{V}_l$ while the integral in the nominator is over all space, i.e. $\mathscr{V}_{l+d} = \mathscr{V}_l + \mathscr{V}_d$. Introducing the displacement field $|D_m\rangle = \epsilon |E_m\rangle$ we may rewrite the result as

$$\Delta\omega_m = -\frac{i}{2}\,\omega_D \times f_m, \quad f_m \equiv \frac{\langle E_m | D_m \rangle_{\mathscr{V}_l}}{\langle E_m | D_m \rangle_{\mathscr{V}_{l+d}}} \qquad (4)$$

where f_m is the fraction of dielectric energy localized in the liquid. Obviously, f_m is a key parameter for refractometry applications of liquid–infiltrated photonic crystals. For void–like structures in the evanescent field sensing limit, f will be of the order of a few percent, while for pillar–like structures the optical overlap with the liquid can be larger than 50%, thus facilitating a much higher sensitivity to refractive index changes in the liquid [9]. For Beer–Lambert–Bouguer absorbance cells, the slow–light enhancement also quite naturally scales with f [14].

In this paper we will explore two consequences of the small imaginary shift in the frequency caused by the small imaginary Ohmic term in Eq. (1). One first obvious consequence is of course the Ohmic damping. Mathematically, the imaginary shift in frequency may via the chain–rule be transformed into a small imaginary shift $\Delta\kappa$ in the Bloch wave vector κ. The corresponding damping parameter $\alpha = 2\Delta\kappa$ of the Bloch modes then becomes

$$\alpha = \frac{f\omega_D}{v_g} \qquad (5)$$

where $v_g = \partial\omega/\partial\kappa$ is the unperturbed group velocity. The attenuation will thus quite intuitively increase with a slowing down of the electromagnetic mode near photonic–band edges. Modes with a large optical overlap with the liquid of course suffer most from Ohmic dissipation as reflected by the proportionality of α to f.

Another consequence of the Ohmic conduction is reflected in the photonic density of states. Quite intuitively, dissipation is linked to a life–time broadening of the electromagnetic states and in the density of states this leads to a smearing of sharp features and even an induced density of states in the gaps where no states exist in the absence of conduction. To see this explicitly we start from the following definition of the density of states

$$\rho(\omega) \propto \int_{\mathscr{V}_{l+d}} dr \operatorname{Im}\{\omega \operatorname{Tr} G(r,r,\omega)\} \qquad (6)$$

where G is the Green's tensor [16, 17] defined in accordance with Eq. (2) and the trace is to sum over the three directions. The density of states is of particular interest to dipole radiation from e.g. excited bio–molecules dissolved in the liquid where the decay rate of the excited state of the molecule is proportional to the electromagnetic density of states. From the Green's tensor G we get the standard result

$$\rho(\omega) = \frac{1}{\mathscr{V}_{BZ}} \sum_m \int_{BZ} d\kappa \frac{2}{\pi} \operatorname{Im}\left\{ \frac{\omega}{\omega^2 - \omega_m^2(\kappa) + i\eta^+} \right\} \qquad (7)$$

with an infinitesimal broadening by η^+ of the electromagnetic levels. The normalization is given by the volume $\mathscr{V}_{BZ} = \int_{BZ} d\kappa$ of the first Brillouin zone. For a vanishing σ the eigenfrequencies ω_m are real and we get the well–known expression

$$\rho_0(\omega) = \frac{1}{\mathscr{V}_{BZ}} \sum_m \int_{BZ} d\kappa \, \delta \left[\omega - \omega_m(\kappa) \right] \qquad (8)$$

where $\delta(x)$ is the Dirac delta function. For a small but finite σ, first–order perturbation theory in the frequency squared (first order in ω_D) gives $\Delta(\omega_m^2) = -i\omega_m\omega_D f$ so that

$$\rho(\omega) = \frac{1}{\mathscr{V}_{BZ}} \sum_m \int_{BZ} d\kappa \frac{2}{\pi} \operatorname{Im}\left\{ \frac{\omega}{\omega^2 - \omega_m^2(\kappa) + i\omega_D\omega_m(\kappa)f_m(\kappa)} \right\} \qquad (9)$$

corresponding to a finite broadening of the order ω_D. Note how some states are broadened more than others depending on the filling fraction and eigenfrequency.

Along with the broadening there will be an induced density of states ρ_{PBG} in the band–gaps where no states were available in the absence of conduction. To see this we consider the center of a band–gap of width $\Delta\Omega$. The induced density–of–states originates mainly from the upper and lower band edges with the frequency and the filling factor evaluated at the edge of the Brillouin zone. From the corresponding tails we get the following for the induced density of states

$$\rho_{PBG} \propto \frac{\omega_D}{(\Delta\Omega)^2} \qquad (10)$$

demonstrating the competition between the two frequency scales given by the Debye frequency and the with of the band gap.

3 NUMERICAL RESULTS

In following we illustrate the above general results by numerical simulations for a particular photonic crystal structure. For the simulations of Eq. (2) we employ a freely available plane–wave method [18]. As an example we consider the TM modes of a square lattice of high–index rods with diameter $d/\Lambda = 0.4$ and $\epsilon_d = 10.5$ and for the liquid $\epsilon_l = (1.33)^2$, see panel (c) in Figure 1. Panel (a) shows the band structure and the corresponding density of states is shown in panel (b) for different values of the Debye frequency. The overall effect of the conductivity is obviously to smear out sharp features as well as to introduce states in the band–gap region of the unperturbed problem, see panel (d).
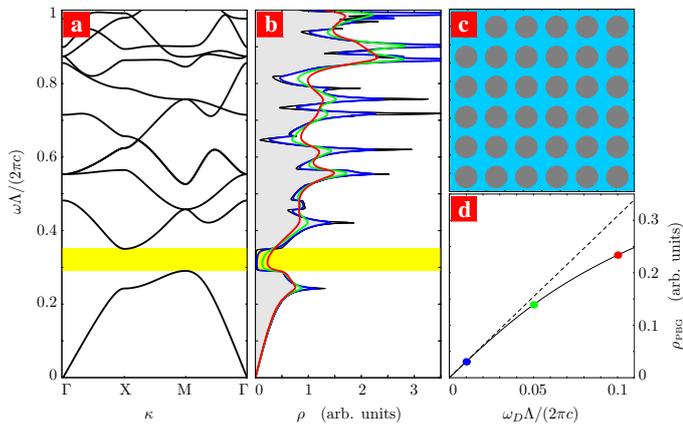
FIG. 1 Liquid infiltrated photonic crystal, see Panel (c), with a square lattice of high-index rods with diameter $d/\Lambda = 0.4$ and $\varepsilon_d = 10.5$ and for the liquid $\varepsilon_l = (1.33)^2$. Panel (a) shows the photonic band structure for TM modes along the high-symmetry directions in the 1st Brillouin zone and panel (b) shows the corresponding photonic density of states. The filled curve shows the density of states in the absence of conduction while the superimposed curves are for $\omega_D\Lambda/(2\pi c) = 0.01$, 0.05, and 0.1. Panel (d) shows the induced density of states in the center of the photonic band gap. The data points correspond to the superimposed curves in panel (b).

In Figure 2 we consider a line–defect waveguide structure where a single line of rods has been removed. Panel (a) shows the dispersion of the waveguide mode (blue solid line). As indicated by the color shading, broadening of the mode is more pronounced near the band edges compared to the central part of the band. Panel (b) shows a corresponding increase in Ohmic attenuation near the mode–band edges. For naturally occurring electrolytes the attenuation will be of the order dB/cm in the center of the band while highly purified water will result in an almost negligible attenuation.

4 CONCLUSION

In conclusion we have studied the influence of Ohmic dissipation on the attenuation and level broadening in liquid–infiltrated photonic crystals. Our general results may readily be applied to other types of liquid–infiltrated photonic crystals such as three–dimensional opal structures as well as quasi two–dimensional membrane structures. Our results illustrate that attention should be paid to Ohmic dissipation and broadening for opto–fluidic applications of photonic crystals in e.g. lab–on–a–chip systems. One quite interesting consequence is the influence of the electrolyte conductivity on the decay dynamics of excited bio–molecules dissolved in the electrolyte. Similarly to the observations for quantum dots in ordinary photonic crystals [19], we expect that spontaneous emission rates of bio–molecules can both be either suppressed (in band–gap regions) or enhanced (e.g. by van Hove singularities) depending on the lattice parameter and the photonic crystal design. Potentially, the latter could be used to enhance inherently weak signals of liquid–dissolved bio–molecules. Strong spectral features in the density–of–states are a necessary condition for this and the present work addresses the degree of persistence of such features in the case of typical electrolytes.

ACKNOWLEDGMENTS

FIG. 2 Liquid infiltrated line–defect photonic crystal waveguide with a square lattice of high-index rods, see Panel (c), with diameter $d/\Lambda = 0.4$ and $\varepsilon_d = 10.5$ while for the liquid $\varepsilon_l = (1.33)^2$. Panel (a) shows the photonic band structure (blue solid line) for propagation of TM polarized light along the ΓX direction in the line–defect waveguide. The color shading indicates the broadening of the line due to a finite conductivity while the grey shading indicates the finite density–of–states in the photonic crystal due to the projected bands in the Brillouin zone. Panel (b) shows the Ohmic attenuation for two different values of the conductivity corresponding to highly purified water (dashed line) and typical drinking water (solid line). The right y–axis shows the results in terms of the free-space wavelength when results are scaled to a structure with $\Lambda = 420\,\text{nm}$. Panel (c) shows the electrical field of the waveguide mode at the Γ-point $\kappa = 0$.

References

[1] D. Psaltis, S. R. Quake, and C. H. Yang, "Developing optofluidic technology through the fusion of microfluidics and optics" Nature **442**, 381 – 386 (2006).

[2] M. Lončar, A. Scherer, and Y. M. Qiu, "Photonic crystal laser sources for chemical detection" Appl. Phys. Lett. **82**, 4648 – 4650 (2003).

[3] E. Chow, A. Grot, L. W. Mirkarimi, M. Sigalas, and G. Girolami, "Ultracompact biochemical sensor built with two–dimensional photonic crystal microcavity" Opt. Lett. **29**, 1093 – 1095 (2004).

[4] P. Domachuk, H. C. Nguyen, B. J. Eggleton, M. Straub, and M. Gu, "Microfluidic tunable photonic band–gap device" Appl. Phys. Lett. **84**, 1838 – 1840 (2004).

[5] H. Kurt and D. S. Citrin, "Coupled–resonator optical waveguides for biochemical sensing of nanoliter volumes of analyte in the terahertz region" Appl. Phys. Lett. **87**, 241119 (2005).

[6] M. L. Adams, M. Lončar, A. Scherer, and Y. M. Qiu, "Microfluidic integration of porous photonic crystal nanolasers for chemical sensing" IEEE J. Sel. Areas Commun. **23**, 1348 – 1354 (2005).

[7] D. Erickson, T. Rockwood, T. Emery, A. Scherer, and D. Psaltis, "Nanofluidic tuning of photonic crystal circuits" Opt. Lett. **31**, 59 – 61 (2006).

[8] T. Hasek, H. Kurt, D. S. Citrin, and M. Koch, "Photonic crystals for fluid sensing in the subterahertz range" Appl. Phys. Lett. **89**, 173508 (2006).

[9] S. Xiao and N. A. Mortensen, "Highly dispersive photonic band–gap–edge optofluidic biosensors" J. Eur. Opt. Soc., Rapid Publ. **1**, 06026 (2006).

[10] E. Yablonovitch, "Inhibited spontaneous emission in solid state physics and electronics" Phys. Rev. Lett. **58**, 2059–2062 (1987).

[11] S. John, "Strong localization of photons in certain disordered dielectric superlattices" Phys. Rev. Lett. **58**, 2486 – 2489 (1987).

[12] T. M. Squires and S. R. Quake, "Microfluidics: Fluid physics at the nanoliter scale" Rev. Mod. Phys. **77**, 977 – 1026 (2005).

[13] G. M. Whitesides, "The origins and the future of microfluidics", Nature **442** 368 – 373 (2006).

[14] N. A. Mortensen and S. Xiao, "Slow–light enhancement of Beer–Lambert–Bouguer absorption", preprint (2006).

[15] N. A. Mortensen, L. H. Olesen, L. Belmon, and H. Bruus, "Electro-hydrodynamics of binary electrolytes driven by modulated surface potentials" Phys. Rev. E **71**, 056306 (2005).

[16] O. J. F. Martin, C. Girard, and A. Dereux, "Generalized field propagator for electromagnetic scattering and light confinement", Phys. Rev. Lett. **74** 526 – 529 (1995).

[17] O. J. F. Martin, C. Girard, D. R. Smith, and S. Schultz, "Generalized field propagator for arbitrary finite–size photonic band gap structures", Phys. Rev. Lett. **82** 315 – 318 (1999).

[18] S. G. Johnson and J. D. Joannopoulos, "Block–iterative frequency–domain methods for Maxwell's equations in a planewave basis", Opt. Express **8** 173 – 190 (2001).

[19] P. Lodahl, A. F. van driel, I. S. Nikolaev, A. Irman, K. Overgaag, D. L. Vanmaekelbergh, and W. L. Vos, "Controlling the dynamics of spontaneous emission from quantum dots by photonic crystals", Nature **430** 654 – 657 (2004).